
GSPRec: Temporal-Aware Graph Spectral Filtering for Recommendation

Ahmad Bin Rabiah
UC San Diego
abinrabiah@ucsd.edu

Julian McAuley
UC San Diego
jmcauley@eng.ucsd.edu

Abstract

Graph-based recommendation systems are effective at modeling collaborative patterns but often suffer from two limitations: overreliance on low-pass filtering, which suppresses user-specific signals, and omission of sequential dynamics in graph construction. We introduce GSPRec, a graph spectral model that integrates temporal transitions through sequentially-informed graph construction and applies frequency-aware filtering in the spectral domain. GSPRec encodes item transitions via multi-hop diffusion to enable the use of symmetric Laplacians for spectral processing. To capture user preferences, we design a dual-filtering mechanism: a Gaussian bandpass filter to extract mid-frequency, user-level patterns, and a low-pass filter to retain global trends. Extensive experiments on four public datasets show that GSPRec consistently outperforms baselines, with an average improvement of 6.77% in NDCG@10. Ablation studies show the complementary benefits of both sequential graph augmentation and bandpass filtering.

1 Introduction

Graph-based recommender systems are constrained by two core problems: using low-pass spectral filtering often suppresses distinct user signals in favor of broad popularity patterns, and the order of user interactions is typically neglected in their graph structures. Therefore, recommender systems should leverage both collaborative patterns and the rich temporal signals embedded within these interaction sequences [19]. Graph-based Collaborative Filtering (CF) methods [14, 42, 49] have achieved strong performance, but they face two limitations. First, models such as LightGCN [14], which rely on linear embedding propagation, act as low-pass filters [42, 33] by smoothing signals across the user-item graph, which encourages popularity but obscures *user-specific patterns* critical for personalization [3]. Second, while some GCN-based recommenders incorporate temporal data, they do so via separate sequential modeling components [26, 16] or by methods that do not integrate order into the graph structure for spectral analysis, which means they still discard *sequential information* needed to distinguish user preferences from popularity patterns [25, 42, 52, 38, 55].

The filtering behavior inherent in many GCNs motivates a closer look through the lens of Graph Signal Processing (GSP), which generalizes classical signal processing to data defined on irregular graph structures [43, 34]. A core technique in GSP is spectral filtering, which transforms graph signals using the eigenbasis of the graph Laplacian [20]. Lowpass filters, which retain only low-frequency components, are widely adopted under the assumption that graph signals are typically smooth [43, 42, 14]. However, mid- and high-frequency components often encode task-relevant, localized, or personalized variations [7, 46, 17] motivating the design of spectral filters that can selectively amplify non-smooth components. Despite GSP’s potential, its adoption in recommender systems [25, 53, 52, 42] has largely focused on lowpass filtering to capture popular preference patterns, overlooking user-specific patterns.

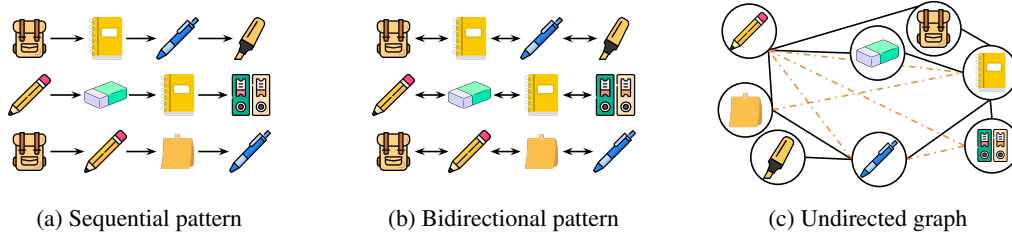


Figure 1: (a) Unidirectional transitions in models like RNNs [15, 18] process items in strict temporal order. (b) Bidirectional models such as BERT4Rec [45] allow context flow in both directions, but only between adjacent items. (c) Undirected item graph from user sequences. Solid lines show the initial symmetric graph S' . Orange dashed lines indicate higher-order relationships learned via multi-hop diffusion (Eq. 2) on S' , which aggregates weighted sequential paths (α and d). The strength of sequence-based connections between items, derived from the aggregated weighted paths of the diffusion process, is reflected in these symmetric links, making the graph ready for spectral filtering. *This sequence is a running example to illustrate graph construction and transition modeling.*

To overcome these limitations, we introduce **GSPRec**, a novel GSP-based framework. GSPRec achieves temporal awareness in spectral recommenders through two components: First, its *sequentially-aware graph construction* encodes multi-hop item transition patterns from user histories via diffusion into a symmetric graph structure, making temporal dynamics an intrinsic property for spectral analysis. Second, this graph empowers a *frequency-aware dual-filtering*, featuring a Gaussian bandpass filter to isolate vital mid-frequency user-specific preferences, complemented by a low-pass filter for popularity patterns.

In this work, we encode the interaction graph with item-to-item transitions derived from user interaction sequences. A multi-hop diffusion process with exponential decay captures sequential dependencies while preserving the benefits of symmetric graph structures. These symmetric structures ensure real eigenvalues and orthogonal eigenvectors [6], which are crucial for stable spectral decomposition and well-defined filtering operations [34]. Unlike prior work that infers item-item similarity from collaborative information [53], our approach aggregates explicit sequential signals into the graph topology. Figure 1 illustrates this shift from sequence-based to graph-based modeling.

Moreover, we design a Gaussian bandpass filter tailored to recommendation graphs. Informed by empirical spectral energy distributions [38, 46], the filter selectively captures *mid-frequency components* that are often associated with user-specific and sequential patterns positioned between low-frequency popularity signals and high-frequency noise. The Gaussian profile provides optimal localization in both spectral and vertex domains [43, 34], which enables smooth transitions across frequencies and reduces ringing artifacts commonly introduced by sharp filter cutoffs [12]. We summarize our contributions as follows:

- We propose a novel graph construction method that first derives a symmetric item connectivity graph from user sequences, then encodes higher-order sequential dependencies via multi-hop diffusion on this symmetric structure.
- We propose a Gaussian bandpass filter that targets mid-frequency components.
- We provide theoretical analysis establishing the stability and convergence of our sequential diffusion and filtering mechanisms.
- We validate our framework on four public benchmarks, showing that integrating sequential transitions with mid-frequency filtering leads to consistent performance gains over baselines.

GSPRec achieves average gains of 6.77% in NDCG@10 and 14.88% in MRR@10 across four public benchmark datasets, consistently outperforming state-of-the-art baselines. These results highlight the effectiveness of our two core design choices: sequential graph encoding and spectral filtering.

2 Related Work & Background

Graph-Based Collaborative Filtering: Graph-based collaborative filtering represents users and items as nodes in a bipartite graph, modeling interactions through various approaches [14, 49,

Table 1: Comparison with existing popular methods.

Method	Task	Spectral Filtering	Temporal Info.	Graph Structure	Message Passing	Mid-Freq
<i>Message Passing GCNs:</i>						
NGCF [49]	General	✗	✗	User-Item	✓	✗
LightGCN [14]	General	✗	✗	User-Item	✓	✗
LR-GCCF [4]	General	✗	✗	User-Item	✓	✗
IMP-GCN [23]	General	✗	✗	User-Item	✓	✗
<i>Spectral Filtering Methods (GSP-based):</i>						
GF-CF [42]	General	LP	✗	User-Item	✗	✗
PGSP [25]	General	LP	✗	User-Item	✗	✗
HiGSP [53]	General	LP	✗	User-Item	✗	✗
FaGSP [52]	General	LP	✗	User-Item	✗	✗
<i>Non-Propagative / Simplified Methods:</i>						
SimpleX [28]	General	✗	✗	User-Item	✗	✗
UltraGCN [29]	General	ApproxLP	✗	User-Item	✗	✗
<i>Sequential Recommendation:</i>						
BERT4Rec [45]	Sequential	✗	✓	Sequence	✗	✗
SASRec [18]	Sequential	✗	✓	Sequence	✗	✗
GSPRec (Ours)	General	BP+LP	✓	UI+Seq	✗	✓

55, 60, 17, 59]. Recent works address challenges including over-smoothing [3, 42], popularity bias [58], representation collapse [36], fairness [2, 56], and efficiency [22, 51], while others improve representations through disentanglement [50, 39, 9] or architectural simplification [29, 28]. Temporal dynamics have been incorporated through sequential models [18, 45, 21] or temporal graphs [57, 35]. Our approach encodes temporal locality directly as edge-level structure and applies spectral filtering without message passing.

Background on Graph Signal Processing: Graph Signal Processing (GSP) analyzes signals on graph structures [34, 43, 40]. A *graph signal* maps values to nodes $\mathcal{G} = (\mathcal{V}, \mathcal{E})$ as $\mathbf{x} \in \mathbb{R}^{|\mathcal{V}|}$. The normalized Laplacian $\mathbf{L} = \mathbf{I} - \mathbf{D}^{-1/2}\mathbf{A}\mathbf{D}^{-1/2}$ decomposes into eigenvalues $\mathbf{\Lambda}$ and eigenvectors \mathbf{U} [6], forming the graph Fourier basis. Spectral filtering transforms signals:

$$\mathbf{x}' = \mathbf{U}g(\mathbf{\Lambda})\mathbf{U}^T\mathbf{x}, \quad \text{where } g(\mathbf{\Lambda}) = \text{diag}(g(\lambda_1), \dots, g(\lambda_n)) \quad (1)$$

Low-pass filters preserve global patterns, while band-pass filters capture mid-frequency variations related to user-specific behavior [34, 12]. In our context, user preference signals and item transition patterns enable spectral analysis as an alternative to neighborhood aggregation.

Graph Signal Processing in Recommendation: Prior work has adapted GSP to recommender systems by treating interactions as graph signals [17, 27, 25, 52, 53, 61, 38]. These approaches employ low-pass filtering for global trends, neglecting mid-frequency components where user-specific patterns often reside. Various methods integrate spectral principles with neural architectures [52, 48, 54] or explore parameter-free formulations [24]. Our approach combines band-pass and low-pass filtering with temporal structure encoding, drawing from classical GSP filter design [20, 46, 30].

3 GSPRec

GSPRec consists of a sequential graph encoding procedure and a frequency-aware spectral filtering framework. These components jointly capture two complementary signal patterns in the spectral domain: (1) globally consistent preference trends across the entire user-item graph, and (2) user-specific variation patterns that distinguish individual preferences. Figure 2 summarizes the pipeline from user-item interactions to final recommendations via graph construction and spectral filtering.

3.1 Problem Formulation

Let $\mathcal{U} = \{u_1, \dots, u_m\}$ denote users and $\mathcal{I} = \{i_1, \dots, i_n\}$ denote items. Historical interactions are triplets $\mathcal{D} = \{(u, i, t) \mid u \in \mathcal{U}, i \in \mathcal{I}, t \in \mathbb{R}^+\}$, yielding binary matrix $\mathbf{X} \in \{0, 1\}^{m \times n}$ where $x_{ui} = 1$ if user u interacted with item i . For each user u , we define a time-ordered sequence $\mathcal{S}_u = [i_1, i_2, \dots]$ where $(u, i_j, t_j) \in \mathcal{D}$ and $t_1 < t_2 < \dots$. Our task is to predict future user-item

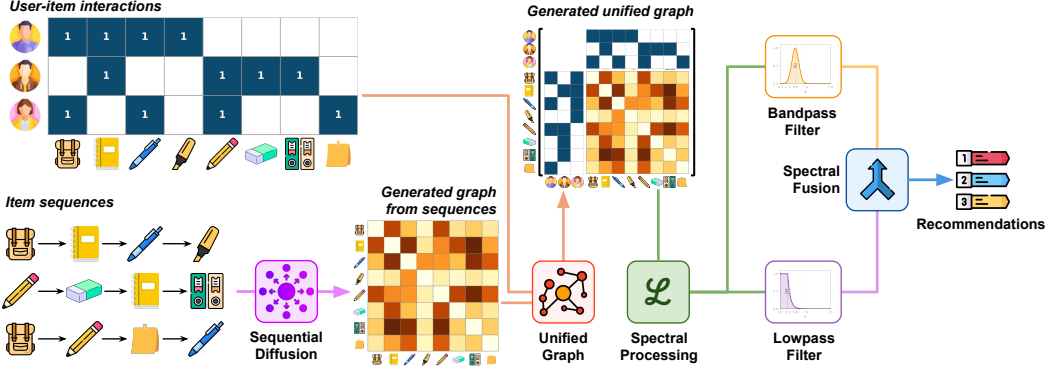


Figure 2: Overview of GSPRec. Starting from user-item interaction sequences (left), we construct a unified graph joining user-item links and item-item transitions via multi-hop diffusion with exponential decay (Eq. 2). This graph is processed using two complementary spectral filters: a band-pass filter to extract mid-frequency, user-specific patterns, and a low-pass filter to capture global trends.

interactions by jointly modeling collaborative patterns and sequential dynamics. Specifically, we aim to predict unobserved entries in \mathbf{X} using a unified spectral graph approach that leverages both user preference similarities and temporal item transitions.

3.2 Recommendation Graph Construction

Our goal is to construct a unified graph that integrates collaborative filtering signals with sequential transition patterns. This allows us to employ spectral methods to model both long-term user preferences and short-term sequential behavior, which typically require symmetric graph Laplacians [6]. The core challenge is to meaningfully translate inherently directed user sequences into a symmetric item-item graph component, denoted $\tilde{\mathbf{S}}$, suitable for this unified spectral analysis.

To achieve this, we shift from traditional sequence modeling paradigms to a graph-based representation that makes temporal dynamics amenable to spectral analysis. Figure 1 illustrates this conceptual shift: unlike models that process sequences directly through (a) unidirectional or (b) locally bidirectional mechanisms, our approach transforms user interaction sequences into (c) an undirected item graph. This graph is constructed to embed sequence-derived item proximity into a symmetric structure, a critical step for enabling spectral methods that typically require such symmetry. Although sequential models excel at capturing ordered context, our graph-based formulation is designed for compatibility with spectral analysis on symmetric matrices. This enables joint analysis of collaborative and sequential signals and decomposition with well-defined spectral properties [20]. However, using directed graphs directly with spectral methods would necessitate asymmetric Laplacians [5], which have different theoretical/computational aspects beyond our current scope. To create the symmetric item-item graph component $\tilde{\mathbf{S}}$ from sequences, we follow the following process.

Initial Symmetric Sequence Graph (\mathbf{S}'): We define an initial directed transition matrix $\mathbf{S} \in \{0, 1\}^{n \times n}$, where $s_{ij} = 1$ if item i directly precedes item j in any user sequence. To adapt this for symmetric spectral methods, we form its undirected version, $\mathbf{S}' \in \{0, 1\}^{n \times n}$. In \mathbf{S}' , an undirected edge (i, j) exists if a transition $i \rightarrow j$ or $j \rightarrow i$ is in \mathbf{S} . This symmetrization is a standard practice when preparing directed graph for algorithms requiring undirected structures [47, 41]. While simplifying transition directionality, this approach allows capturing broader item relatedness from sequences, as rigid order is not always optimal and wider context can be beneficial [45]. Multi-hop diffusion (Eq. 2) operates on \mathbf{S}' to encode sequence-derived item associations.

Multi-Hop Diffusion ($\mathbf{S}^{(d)}$): While \mathbf{S}' captures direct sequential links to model broader item influence propagated through multi-step paths within this symmetrized sequence-derived structure, we apply multi-hop diffusion directly to the symmetric graph \mathbf{S}' :

$$\mathbf{S}^{(d)} = \sum_{k=1}^d \alpha^{k-1} (\mathbf{S}')^k \quad (2)$$

where $\alpha \in (0, 1)$ is an exponential decay factor that gives higher weight to shorter paths in \mathbf{S}' , thus emphasizing local sequential relationships. d is the diffusion depth to control the extent of influence propagation. Since \mathbf{S}' is symmetric, each power $(\mathbf{S}')^k$ is symmetric, and therefore the diffused matrix $\mathbf{S}^{(d)}$ is also symmetric. The entries $S_{ij}^{(d)}$ represent a score of multi-hop, locality-aware proximity between items i and j , learned from the aggregated sequential patterns as illustrated in Figure 3. This diffusion process is analogous to using graph diffusion kernels to define similarity [10] and converges when $\alpha < 1/\rho(\mathbf{S}')$.

Lemma 1 (Diffusion Convergence). *The diffusion process defined in Eq. 2 converges as $d \rightarrow \infty$ if $\alpha < 1/\rho(\mathbf{S}')$, where $\rho(\cdot)$ denotes the spectral radius of \mathbf{S}' .*

Proof. The diffusion process as $d \rightarrow \infty$ is $\mathbf{S}^{(\infty)} = \sum_{k=1}^{\infty} \alpha^{k-1} (\mathbf{S}')^k$. We can rewrite this as $\mathbf{S}^{(\infty)} = \mathbf{S}' \sum_{j=0}^{\infty} (\alpha \mathbf{S}')^j$ by letting $j = k - 1$. This series converges if the standard matrix geometric series $\sum_{j=0}^{\infty} M^j$, where $M = \alpha \mathbf{S}'$, converges. This occurs if the spectral radius $\rho(M) < 1$, i.e., $\rho(\alpha \mathbf{S}') < 1$. Since $\rho(\alpha \mathbf{S}') = \alpha \rho(\mathbf{S}')$ (for $\alpha > 0$), convergence requires $\alpha < 1/\rho(\mathbf{S}')$. \square

In practice, we estimate $\rho(\mathbf{S}')$ (e.g., via power iteration) and choose a suitable α .

Symmetric Normalization ($\tilde{\mathbf{S}}$): The resulting symmetric, diffused matrix $\mathbf{S}^{(d)}$ is then symmetrically normalized to produce the final item-item graph component:

$$\tilde{\mathbf{S}} = \mathbf{D}_S^{-1/2} \mathbf{S}^{(d)} \mathbf{D}_S^{-1/2}, \quad \text{where } \mathbf{D}_S = \text{diag}(\mathbf{S}^{(d)} \mathbf{1}_n) \quad (3)$$

This standard normalization technique [6] yields $\tilde{\mathbf{S}}$, ensuring its weights are scaled appropriately for stable spectral analysis. The weights in $\tilde{\mathbf{S}}$ reflect a transformation of user sequences into measures of item-item sequential relevance.

Interaction Normalization: The raw user-item interaction matrix \mathbf{X} is normalized to account for varying user activity levels and popularities of the items. Standard normalizations include:

$$\tilde{\mathbf{X}}_U = \mathbf{D}_U^{-1/2} \mathbf{X}, \quad \tilde{\mathbf{X}}_I = \mathbf{X} \mathbf{D}_I^{-1/2} \quad (4)$$

where $\mathbf{D}_U = \text{diag}(\mathbf{X} \mathbf{1}_n)$ and $\mathbf{D}_I = \text{diag}(\mathbf{X}^T \mathbf{1}_m)$. For constructing the unified adjacency matrix \mathbf{A} , we use the original binary interaction matrix \mathbf{X} , as its structure is fundamental. The normalized versions can be used in other components, like the filter design.

Unified Graph Adjacency and Laplacian

(A, L): We integrate the user-item interactions \mathbf{X} and the sequence-derived item-item graph $\tilde{\mathbf{S}}$ into a single, symmetric adjacency matrix for the unified graph:

$$\mathbf{A} = \begin{bmatrix} \mathbf{0}_{m \times m} & \mathbf{X} \\ \mathbf{X}^T & \tilde{\mathbf{S}} \end{bmatrix} \quad (5)$$

This matrix \mathbf{A} forms a heterogeneous graph where the $\mathbf{0}_{m \times m}$ block denotes no direct user-user links are explicitly modeled here, \mathbf{X} captures user-item interactions, and $\tilde{\mathbf{S}}$ encodes the sequence-derived item-item relationships. From \mathbf{A} , we compute the symmetric normalized Laplacian, which is the cornerstone of our spectral filtering:

$$\mathbf{L} = \mathbf{I} - \mathbf{D}^{-1/2} \mathbf{A} \mathbf{D}^{-1/2}, \quad \text{where } \mathbf{D} = \text{diag}(\mathbf{A} \mathbf{1}) \quad (6)$$

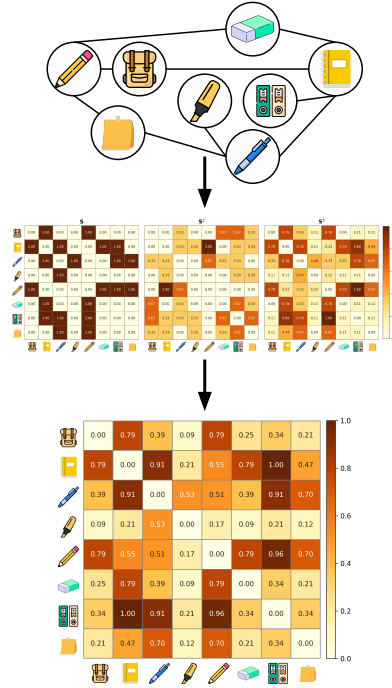


Figure 3: Multi-hop diffusion (Eq. 2) on the symmetric base graph \mathbf{S}' (derived from initial directed sequences) with $\alpha = 0.5$. Top: \mathbf{S}' . Middle: Powers $(\mathbf{S}')^k$. Bottom: $\mathbf{S}^{(3)}$ encoding decayed proximity.

The properties of this Laplacian are discussed in Proposition 2. Our approach, by constructing $\tilde{\mathbf{S}}$ from symmetrized sequential data and then applying diffusion, embeds sequence-derived proximity into a standard spectral framework, offering a distinct way to leverage temporal signals compared to pure sequential models that maintain strict causality [15, 18, 45].

Proposition 2 (Laplacian Validity). *The Laplacian \mathbf{L} , constructed from the symmetric adjacency matrix \mathbf{A} , is symmetric, positive semidefinite, and has real eigenvalues in the range $[0, 2]$.*

Proof sketch; full proof in Appendix B. This follows from spectral graph theory [6], as \mathbf{A} is constructed to be symmetric and non-negative, and Eq. 6 defines the standard normalized Laplacian. \square

3.3 Spectral Filtering Framework

To model user preferences at different levels of specificity, we perform spectral filtering on the Laplacian graph $\mathbf{L} = \mathbf{U}\mathbf{\Lambda}\mathbf{U}^T$ where $\mathbf{\Lambda} = \text{diag}(\lambda_1, \dots, \lambda_{m+n})$ contains eigenvalues in ascending order $0 \leq \lambda_1 \leq \lambda_2 \leq \dots \leq \lambda_{m+n} \leq 2$ and $\mathbf{U} = [\mathbf{u}_1, \dots, \mathbf{u}_{m+n}]$ contains the corresponding eigenvectors. In practice, for computational efficiency, we perform a truncated eigendecomposition focusing on $r \ll (m+n)$ which includes the low- and mid-frequency bands relevant to our filters. The lowpass filter $g_{LP}(\lambda)$ and bandpass filter $g_{BP}(\lambda)$ operate on the corresponding r eigenpairs by selecting and amplifying the mid-frequency signals present within this subspace.

Proposition 3 (Laplacian Properties). *The eigenvalues of \mathbf{L} lie in $[0, 2]$, with the number of zero eigenvalues equal to the number of connected components in the graph.*

Bandpass Filtering: To capture mid-frequency user-specific behavior, we design a bandpass filter to the graph spectrum using a Gaussian kernel:

$$g_{BP}(\lambda) = \exp\left(-\frac{(\bar{\lambda} - c)^2}{w}\right), \quad \bar{\lambda} = \frac{\lambda - \lambda_{\min}}{\lambda_{\max} - \lambda_{\min}} \quad (7)$$

where c and w control the center and width of the frequency band. This form is motivated by our empirical analysis (Appendix G), which indicates that spectral coefficients for intermediate eigenvalues often show higher magnitude for user-specific preferences compared to global trends. Let $\mathbf{G}_{BP} = \text{diag}(g_{BP}(\lambda_1), \dots, g_{BP}(\lambda_r))$ denote the spectral bandpass filter. We filter the item-degree-normalized user-item interaction signal using the band-pass operator:

$$\mathbf{F}_{BP} = \mathbf{X}\mathbf{D}_I^{-1/2}\mathbf{U}\mathbf{G}_{BP}\mathbf{U}^T\mathbf{D}_I^{-1/2} \quad (8)$$

Lowpass Filtering: To preserve global structure and smooth preferences, we compute a complementary low-pass component augmented with user-user similarity. To enhance global structure, we augment user-item signals with user-user similarities. We define $\mathbf{X}_b = [\mathbf{C}_U, \mathbf{X}]$, where $\mathbf{C}_U = \tilde{\mathbf{X}}_U\tilde{\mathbf{X}}_U^T$. The low-pass component is then computed as:

$$\mathbf{F}_{LP} = \mathbf{X}_b\mathbf{D}_b^{-1/2}\mathbf{U}\mathbf{U}^T\mathbf{D}_b^{1/2} \quad (9)$$

where $\mathbf{D}_b = \text{diag}(\mathbf{X}_b^T\mathbf{1}_m)$. We note that \mathbf{C}_U is not part of the Laplacian but is introduced to incorporate global user similarity in the lowpass representation. As \mathbf{X}_b contains both user-user and user-item components, we extract only the item-related part after filtering by:

$$\mathbf{F}_{LP} = \mathbf{F}_{LP}[:, m:] \quad (10)$$

In our framework, mid-frequency components correspond to more user-specific variations, while low frequencies capture smoother, population-level preferences. We compute item scores by fusing mid-frequency personalization with low-frequency global trends. Specifically, we compute:

$$\mathbf{Y} = \phi \cdot \mathbf{F}_{BP} + (1 - \phi) \cdot \mathbf{F}_{LP}, \quad \phi \in [0, 1] \quad (11)$$

From a GSP perspective, both \mathbf{F}_{BP} and \mathbf{F}_{LP} are outputs of linear spectral filters applied to the graph Laplacian \mathbf{L} . Their convex combination remains a valid linear operator, as the space of spectral filters is closed under *addition* and *scalar multiplication* [40, 37]. Figure 2 illustrates our dual-filter architecture. The spectral components separate distinct preference signals: low-frequency components (from lowpass filter) capture common transitions shared across users like the `backpack`→`notebook` association in multiple sequences. Mid-frequency components (from bandpass filter) extract distinctive patterns such as `pencil`→`eraser`→`notebook`→`calculator` sequences that characterize specific user subgroups. Figure 3 shows how our diffusion process captures these sequential patterns, with darker cells indicating stronger connections derived from user histories. Appendix B provides a complete description, with complexity analysis in Appendix D.

4 Experiments

We evaluate GSPRec to answer: (1) How does sequential graph enrichment affect performance? (2) What is the impact of frequency-aware filtering? (3) How does GSPRec compare to state-of-the-art recommenders?

4.1 Setup

Data: We conduct experiments on four benchmark datasets spanning two domains: (1) ML100K, ML1M [13] and Netflix [1] from the movie recommendation domain; (2) Amazon Beauty [32] from the e-commerce product domain. These datasets were selected to maintain comparability with recent spectral methods [52, 53] that established them as standard benchmarks for this class of approaches. All datasets are divided into training set and test set with the ratio of 8:2, and we take 10% of the training set as validation set for hyperparameter tuning. Table 2 shows the statistics of these datasets.

Baselines: We compare GSPRec with: (i) **Popularity**; (ii) GCN-based methods: **LightGCN** [14], **LR-GCCF** [4], **IMP-GCN** [23], **SimpleX** [28], **UltraGCN** [29]; and (iii) GSP-based methods: **GF-CF** [42], **PGSP** [25], **FaGSP** [52], **HiGSP** [53]. A detailed description of these baselines is provided in Appendix E. Unlike existing GSP methods that use only collaborative signals and low-pass filtering, GSPRec encodes temporal transitions into the graph topology and employs a dual-filter approach targeting both low and bandpass filter components.

Implementation Details: For graph construction, we set the diffusion depth $d = 2$ and the decay $\alpha = 0.4$ in all datasets to capture immediate and second-order transitions while attenuating longer-range influences. Eigendecomposition dimensionality r varies by dataset size. Filter parameters c , w , and fusion weight ϕ are tuned per dataset as shown in Table 3. Implementation details are in Appendix F.

Table 2: Statistics of evaluation datasets.

Dataset	#Users	#Items	#Inter.	Density
ML100K	943	1,682	100,000	6.30%
ML1M	6,040	3,706	1,000,209	4.47%
Netflix	20,000	17,720	5,678,654	1.60%
Beauty	22,363	12,101	198,502	0.07%

Table 3: Filter parameters across datasets.

Dataset	ϕ	c	w	r
ML100K	0.5	0.2	0.1	32
ML1M	0.3	0.8	0.1	128
Netflix	0.3	0.4	0.3	256
Beauty	0.5	0.8	0.3	512

Metrics. Following prior work [14, 42, 52, 53, 25], we use Normalized Discounted Cumulative Gain (NDCG@ k) and Mean Reciprocal Rank (MRR@ k) at $k \in \{5, 10, 20\}$. We apply spectral filtering to obtain preference scores, exclude previously interacted items, and rank the top- k items.

4.2 Overall Performance Comparison

Table 4 presents performance comparisons. GSPRec consistently outperforms all baselines across all metrics and datasets. Three Key observations: (1) consistent NDCG@ k /MRR@ k improvements show stronger ranking quality, (2) larger gains on sparse datasets confirm robustness, and (3) improvements over recent GSP-based methods validate the benefit of leveraging both sequential and spectral signals.

4.3 Parameter Study

Sequential-Aware Graph: To isolate the contribution of sequential graph, we compare our full model with four variants shown in Table 5: (1) GSPRec-NB: no band-pass filter, (2) GSPRec-NL: no low-pass filter, (3) GSPRec-NS: no sequential diffusion, (4) GSPRec-SE: sequence edges only (no diffusion). The non-sequential variant (GSPRec-NS) shows significant performance drops, confirming the value of sequential information. The direct-sequence variant (GSPRec-SE) performs slightly worse than the full model, demonstrating that higher-order transitions captured by multi-hop diffusion provide additional benefits.

Table 4: Performance comparison on four public datasets. The best performance is denoted in **bold**. “M@K” and “N@K” are short for “MRR@K” and “NDCG@K”, respectively. “Improv.” denotes the percentage improvement of GSPRec compared to the strongest baseline method.

Datasets	Metric	GCN-based Methods						GSP-based Methods					Improv.
		Popularity	LightGCN	LR-GCCF	IMP-GCN	SimpleX	UltraGCN	GF-CF	PGSP	FaGSP	HiGSP	GSPRec	
ML100K	N@5	0.5672	0.7034	0.5587	0.6764	0.6995	0.6786	0.6875	0.6851	0.7106	0.7166	0.7543	+5.26%
	M@5	0.5151	0.6362	0.4943	0.6006	0.6397	0.6094	0.6234	0.6149	0.6518	<u>0.6629</u>	0.7358	+11.00%
	N@10	0.5857	0.6771	0.5603	0.6605	0.6866	0.6688	0.6843	0.6722	<u>0.7092</u>	0.7021	0.7572	+6.77%
	M@10	0.5296	0.5877	0.4616	0.5690	0.6064	0.5749	0.6010	0.5767	<u>0.6384</u>	0.6380	0.7443	+16.59%
	N@20	0.5867	0.6618	0.5555	0.6605	0.6543	0.6486	0.6621	0.6495	<u>0.6989</u>	0.6724	0.7465	+6.81%
	M@20	0.5315	0.5652	0.4411	0.5690	0.5411	0.5289	0.5593	0.5496	<u>0.5901</u>	0.5782	0.7457	+26.37%
ML1M	N@5	0.0958	0.5845	0.3540	0.5583	0.5934	0.5739	0.5935	0.5963	<u>0.6112</u>	0.6062	0.6237	+2.05%
	M@5	0.1943	0.5160	0.2997	0.4934	0.5244	0.5087	0.5254	0.5313	<u>0.5430</u>	0.5386	0.5715	+5.25%
	N@10	0.0960	0.5873	0.3787	0.5594	0.5921	0.5773	0.5897	0.5923	<u>0.6082</u>	0.6042	0.6431	+5.74%
	M@10	0.2180	0.5010	0.2946	0.4685	0.5051	0.4886	0.4996	0.5063	<u>0.5229</u>	0.5148	0.5837	+11.63%
	N@20	0.1035	0.5692	0.3980	0.5416	0.5687	0.5600	0.5678	0.5687	<u>0.5808</u>	0.5769	0.6431	+10.73%
	M@20	0.2309	0.4644	0.2924	0.4292	0.4625	0.4500	0.4557	0.4646	<u>0.4748</u>	0.4620	0.5871	+23.65%
Netflix	N@5	0.5105	0.6822	0.6023	0.6328	0.6603	0.5680	0.7005	0.6811	<u>0.7162</u>	0.7162	0.7201	+0.54%
	M@5	0.4505	0.6147	0.5323	0.5528	0.5902	0.4941	0.6360	0.6127	<u>0.6524</u>	0.6532	0.6680	+2.27%
	N@10	0.5488	0.6814	0.6134	0.6307	0.6694	0.5746	0.6928	0.6756	<u>0.7079</u>	0.7062	0.7270	+2.70%
	M@10	0.4712	0.5974	0.5234	0.5386	0.5839	0.4708	0.6126	0.5905	<u>0.6293</u>	0.6275	0.6762	+7.45%
	N@20	0.5604	0.6642	0.6043	0.6152	0.6572	0.5580	0.6689	0.6543	<u>0.6814</u>	0.6800	0.7213	+5.86%
	M@20	0.4773	0.5636	0.4963	0.4995	0.5555	0.4309	0.5691	0.5502	<u>0.5827</u>	0.5800	0.6777	+16.30%
Beauty	N@5	0.0149	0.0668	0.0533	0.0570	0.0682	0.0599	0.0659	0.0674	<u>0.0712</u>	0.0718	0.0733	+2.09%
	M@5	0.0118	0.0530	0.0423	0.0444	0.0544	0.0476	0.0523	0.0538	0.0564	<u>0.0574</u>	0.0619	+7.84%
	N@10	0.0200	0.0763	0.0635	0.0667	0.0761	0.0649	0.0751	0.0765	<u>0.0799</u>	0.0771	0.0879	+10.01%
	M@10	0.0139	0.0519	0.0443	0.0451	0.0517	0.0441	0.0517	0.0525	<u>0.0549</u>	0.0531	0.0680	+23.86%
	N@20	0.0256	0.0829	0.0678	0.0729	0.0819	0.0689	0.0819	0.0828	<u>0.0846</u>	0.0799	0.1013	+19.74%
	M@20	0.0154	0.0466	0.0388	0.0409	0.0461	0.0393	0.0469	0.0481	<u>0.0485</u>	0.0456	0.0718	+48.04%

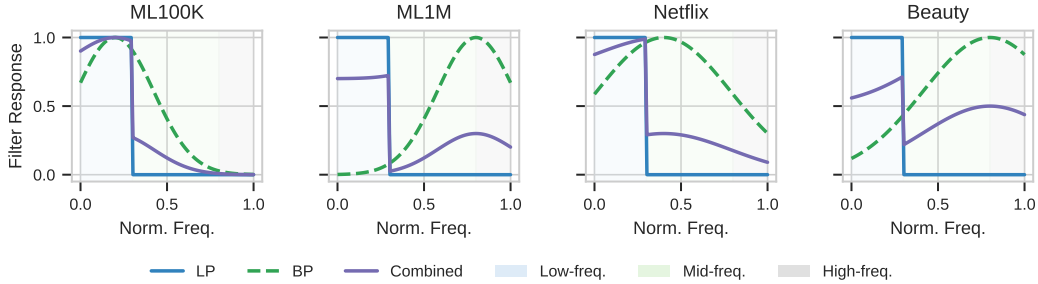


Figure 4: Frequency response curves of different filter configurations all datasets. The low-pass filter (blue) preserves signals in the lower 30% of the spectrum. The band-pass filter (green) selectively amplifies mid-frequency components associated with personalized patterns. The combined filter response (purple) illustrates how dual-filter captures complementary signals across the spectrum.

Table 5: Ablation study on ML1M dataset.

Variant	N@10	± SE	M@10	± SE
GSPRec-NB	0.5769	0.0082	0.5148	0.0093
GSPRec-NL	0.6042	0.0079	0.5229	0.0088
GSPRec-NS	0.6274	0.0039	0.5704	0.0050
GSPRec-SE	0.6416	0.0037	0.5831	0.0049
GSPRec	0.6431	0.0074	0.5837	0.0081

Table 6: Filtering comparison on ML1M dataset.

Components	N@10	± SE	M@10	± SE
F_{LP} only	0.5769	0.0082	0.5148	0.0093
F_{BP} only	0.6042	0.0079	0.5229	0.0088
$F_{LP}+F_{BP}$ ($\phi=0.3$)	0.6431	0.0074	0.5837	0.0081
$F_{LP}+F_{BP}$ ($\phi=0.5$)	0.6327	0.0076	0.5714	0.0085
$F_{LP}+F_{BP}$ ($\phi=0.7$)	0.6281	0.0078	0.5682	0.0087

Spectral Filtering Performance: Table 3 shows optimal filter settings across datasets: (1) larger datasets require higher eigendecomposition dimensions r ; (2) sparser datasets benefit from wider bandpass filters; and (3) fusion weight ϕ correlates with dataset density. Figure 4 illustrates filter frequency responses spanning both global and user-specific bands. As shown in Table 6, the dual-filter approach consistently outperforms single-filter alternatives, with best performance at $\phi=0.3$ on ML1M. Notably, the bandpass filter alone outperforms the lowpass filter alone by 4.7% in N@10 and 1.6% in M@10, highlighting the importance of mid-frequency components for personalization. Ablation results in Table 5 further support this, with GSPRec-NB (no band-pass) showing the largest performance drops.

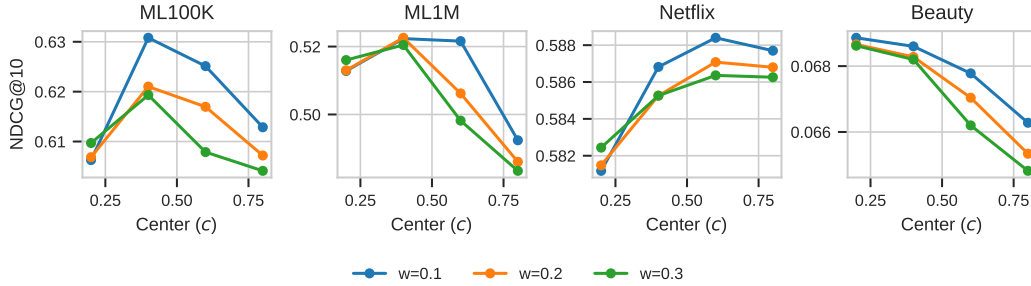


Figure 5: Effect of bandpass center position (c) on NDCG@10 across datasets. Each line represents a different filter bandwidth (w).

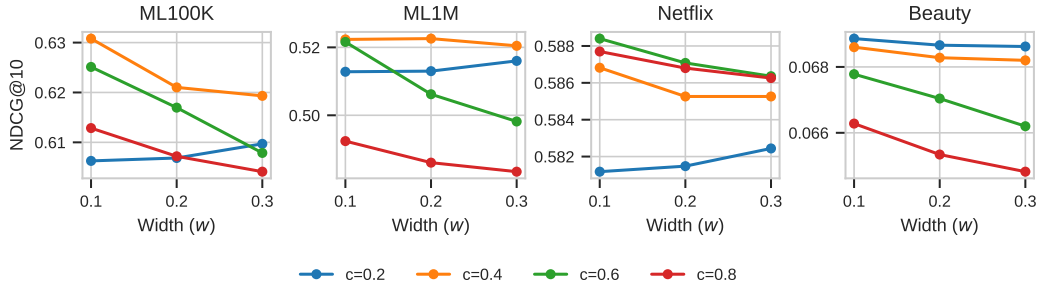


Figure 6: Effect of bandpass width (w) on NDCG@10 across datasets. Each line represents a different center position (c). Optimal width depends on center position and dataset characteristics.

4.4 Parameter Sensitivity Analysis

Figures 5 and 6 show how performance varies with band-pass filter parameters. The center position (c) exhibits dataset-specific optima, reflecting varying spectral distributions across recommendation domains. Filter width (w) interacts with center position. The fusion weight ϕ also shows dataset-dependent patterns: denser datasets favor global signals (lower ϕ), while sparser datasets benefit from stronger mid-frequency personalization (higher ϕ).

5 Conclusion

We introduced GSPRec, a graph-spectral framework that jointly models collaborative and sequential signals via a unified Laplacian. Our method augments the user-item graph with multi-hop, exponentially decayed item transitions and applies dual spectral filters. Theoretically, we ensure spectral convergence and Laplacian validity. Empirically, we demonstrate consistent improvements across four benchmarks over state-of-the-art GSP methods. Ablation studies confirm the necessity of both sequential graph encoding and frequency-aware filtering. Future work includes extending to directed graphs, learning adaptive spectral filters, and applying to diverse recommendation contexts.

6 Broader Impact

This work improves recommender systems by integrating sequential behavior with graph spectral analysis, benefiting users across e-commerce, media, and education domains. However, spectral methods may amplify biases in historical data, potentially reinforcing popularity bias or increasing computational overhead. Future work should explore fairness-aware spectral filters, robustness evaluations, and privacy-preserving techniques. We encourage practitioners to consider these tradeoffs when deploying these systems in real-world settings.

References

- [1] James Bennett and Stan Lanning. The netflix prize. *Proceedings of KDD Cup and Workshop 2007*, pages 3–6, 2007.
- [2] Ludovico Boratto, Francesco Fabbri, Gianni Fenu, Mirko Marras, and Giacomo Medda. Fair augmentation for graph collaborative filtering. In *Proceedings of the 18th ACM Conference on Recommender Systems*, pages 158–168, 2024.
- [3] Deli Chen, Yankai Lin, Wei Li, Peng Li, Jie Zhou, and Xu Sun. Measuring and relieving the over-smoothing problem for graph neural networks from the topological view. In *Proceedings of the AAAI conference on artificial intelligence*, volume 34, pages 3438–3445, 2020.
- [4] Lei Chen, Le Wu, Richang Hong, Kun Zhang, and Meng Wang. Revisiting graph based collaborative filtering: A linear residual graph convolutional network approach. In *Proceedings of the AAAI conference on artificial intelligence*, volume 34, pages 27–34, 2020.
- [5] Fan Chung. Laplacians and the cheeger inequality for directed graphs. *Annals of Combinatorics*, 9:1–19, 2005.
- [6] Fan RK Chung. *Spectral graph theory*, volume 92. American Mathematical Soc., 1997.
- [7] Xiaowen Dong, Dorina Thanou, Michael Rabbat, and Pascal Frossard. Learning graphs from data: A signal representation perspective. *IEEE Signal Processing Magazine*, 36(3):44–63, 2019.
- [8] Charless Fowlkes, Serge Belongie, Fan Chung, and Jitendra Malik. Spectral grouping using the nystrom method. *IEEE transactions on pattern analysis and machine intelligence*, 26(2):214–225, 2004.
- [9] Hao-Ming Fu, Patrick Poirson, Kwot Sin Lee, and Chen Wang. Revisiting neighborhood-based link prediction for collaborative filtering. In *Companion Proceedings of the Web Conference 2022*, pages 1009–1018, 2022.
- [10] Johannes Gasteiger, Stefan Weißenberger, and Stephan Günnemann. Diffusion improves graph learning. *Advances in neural information processing systems*, 32, 2019.
- [11] Nathan Halko, Per-Gunnar Martinsson, and Joel A Tropp. Finding structure with randomness: Probabilistic algorithms for constructing approximate matrix decompositions. *SIAM review*, 53(2):217–288, 2011.
- [12] David K Hammond, Pierre Vandergheynst, and Rémi Gribonval. Wavelets on graphs via spectral graph theory. *Applied and Computational Harmonic Analysis*, 30(2):129–150, 2011.
- [13] F Maxwell Harper and Joseph A Konstan. The movielens datasets: History and context. *Acm transactions on interactive intelligent systems (tiis)*, 5(4):1–19, 2015.
- [14] Xiangnan He, Kuan Deng, Xiang Wang, Yan Li, Yongdong Zhang, and Meng Wang. Lightgcn: Simplifying and powering graph convolution network for recommendation. In *Proceedings of the 43rd International ACM SIGIR conference on research and development in Information Retrieval*, pages 639–648, 2020.
- [15] Balázs Hidasi, Alexandros Karatzoglou, Linas Baltrunas, and Domonkos Tikk. Session-based recommendations with recurrent neural networks. *arXiv preprint arXiv:1511.06939*, 2015.
- [16] Cheng Hsu and Cheng-Te Li. Retaggn: Relational temporal attentive graph neural networks for holistic sequential recommendation. In *Proceedings of the web conference 2021*, pages 2968–2979, 2021.
- [17] Weiyu Huang, Antonio G Marques, and Alejandro Ribeiro. Collaborative filtering via graph signal processing. In *2017 25th European signal processing conference (EUSIPCO)*, pages 1094–1098. IEEE, 2017.
- [18] Wang-Cheng Kang and Julian McAuley. Self-attentive sequential recommendation. In *2018 IEEE international conference on data mining (ICDM)*, pages 197–206. IEEE, 2018.
- [19] Yehuda Koren. Collaborative filtering with temporal dynamics. In *Proceedings of the 15th ACM SIGKDD international conference on Knowledge discovery and data mining*, pages 447–456, 2009.
- [20] Stephen Kruzick and José MF Moura. Graph signal processing: Filter design and spectral statistics. In *2017 IEEE 7th International Workshop on Computational Advances in Multi-Sensor Adaptive Processing (CAMSAP)*, pages 1–5. IEEE, 2017.

- [21] Yaoyiran Li, Xiang Zhai, Moustafa Alzantot, Keyi Yu, Ivan Vulić, Anna Korhonen, and Mohamed Hammad. Calrec: Contrastive alignment of generative llms for sequential recommendation. In *Proceedings of the 18th ACM Conference on Recommender Systems*, pages 422–432, 2024.
- [22] Xurong Liang, Tong Chen, Lizhen Cui, Yang Wang, Meng Wang, and Hongzhi Yin. Lightweight embeddings for graph collaborative filtering. In *Proceedings of the 47th International ACM SIGIR Conference on Research and Development in Information Retrieval*, pages 1296–1306, 2024.
- [23] Fan Liu, Zhiyong Cheng, Lei Zhu, Zan Gao, and Liqiang Nie. Interest-aware message-passing gcn for recommendation. In *Proceedings of the web conference 2021*, pages 1296–1305, 2021.
- [24] Jiahao Liu, Dongsheng Li, Hansu Gu, Tun Lu, Peng Zhang, and Ning Gu. Parameter-free dynamic graph embedding for link prediction. *Advances in Neural Information Processing Systems*, 35:27623–27635, 2022.
- [25] Jiahao Liu, Dongsheng Li, Hansu Gu, Tun Lu, Peng Zhang, Li Shang, and Ning Gu. Personalized graph signal processing for collaborative filtering. In *Proceedings of the ACM Web Conference 2023*, pages 1264–1272, 2023.
- [26] Chen Ma, Liheng Ma, Yingxue Zhang, Jianing Sun, Xue Liu, and Mark Coates. Memory augmented graph neural networks for sequential recommendation. In *Proceedings of the AAAI conference on artificial intelligence*, volume 34, pages 5045–5052, 2020.
- [27] Jeremy Ma, Weiyu Huang, Santiago Segarra, and Alejandro Ribeiro. Diffusion filtering of graph signals and its use in recommendation systems. In *2016 IEEE International Conference on Acoustics, Speech and Signal Processing (ICASSP)*, pages 4563–4567. IEEE, 2016.
- [28] Kelong Mao, Jieming Zhu, Jinpeng Wang, Quanyu Dai, Zhenhua Dong, Xi Xiao, and Xiuqiang He. Simplex: A simple and strong baseline for collaborative filtering. In *Proceedings of the 30th ACM international conference on information & knowledge management*, pages 1243–1252, 2021.
- [29] Kelong Mao, Jieming Zhu, Xi Xiao, Biao Lu, Zhaowei Wang, and Xiuqiang He. Ultragen: ultra simplification of graph convolutional networks for recommendation. In *Proceedings of the 30th ACM international conference on information & knowledge management*, pages 1253–1262, 2021.
- [30] Sunil K Narang, Akshay Gadde, Eduard Sanou, and Antonio Ortega. Localized iterative methods for interpolation in graph structured data. In *2013 IEEE Global conference on signal and information processing*, pages 491–494. IEEE, 2013.
- [31] Mark EJ Newman. Finding community structure in networks using the eigenvectors of matrices. *Physical Review E—Statistical, Nonlinear, and Soft Matter Physics*, 74(3):036104, 2006.
- [32] Jianmo Ni, Jiacheng Li, and Julian McAuley. Justifying recommendations using distantly-labeled reviews and fine-grained aspects. In *Proceedings of the 2019 conference on empirical methods in natural language processing and the 9th international joint conference on natural language processing (EMNLP-IJCNLP)*, pages 188–197, 2019.
- [33] Hoang Nt and Takanori Maehara. Revisiting graph neural networks: All we have is low-pass filters. *arXiv preprint arXiv:1905.09550*, 2019.
- [34] Antonio Ortega, Pascal Frossard, Jelena Kovačević, José MF Moura, and Pierre Vandergheynst. Graph signal processing: Overview, challenges, and applications. *Proceedings of the IEEE*, 106(5):808–828, 2018.
- [35] Zhonghong Ou, Xiao Zhang, Yifan Zhu, Shuai Lyu, Jiahao Liu, and Tu Ao. Ls-tgcn: Long and short-term temporal graph neural network for session-based recommendation. In *Proceedings of the AAAI Conference on Artificial Intelligence*, volume 39, pages 12426–12434, 2025.
- [36] Shaowen Peng, Xin Liu, Kazunari Sugiyama, and Tsunenori Mine. How powerful is graph filtering for recommendation. In *Proceedings of the 30th ACM SIGKDD Conference on Knowledge Discovery and Data Mining*, pages 2388–2399, 2024.
- [37] Markus Püschel and José MF Moura. Algebraic signal processing theory. *arXiv preprint cs/0612077*, 2006.
- [38] Yifang Qin, Wei Ju, Yiyang Gu, Ziyue Qiao, Zhiping Xiao, and Ming Zhang. Polycf: Towards optimal spectral graph filters for collaborative filtering. *ACM Transactions on Information Systems*, 2024.
- [39] Xubin Ren, Lianghao Xia, Jiashu Zhao, Dawei Yin, and Chao Huang. Disentangled contrastive collaborative filtering. In *Proceedings of the 46th international ACM SIGIR conference on research and development in information retrieval*, pages 1137–1146, 2023.

- [40] Aliaksei Sandryhaila and José MF Moura. Discrete signal processing on graphs. *IEEE transactions on signal processing*, 61(7):1644–1656, 2013.
- [41] Venu Satuluri and Srinivasan Parthasarathy. Symmetrizations for clustering directed graphs. In *Proceedings of the 14th international conference on extending database technology*, pages 343–354, 2011.
- [42] Yifei Shen, Yongji Wu, Yao Zhang, Caihua Shan, Jun Zhang, B Khaled Letaief, and Dongsheng Li. How powerful is graph convolution for recommendation? In *Proceedings of the 30th ACM international conference on information & knowledge management*, pages 1619–1629, 2021.
- [43] David I Shuman, Sunil K Narang, Pascal Frossard, Antonio Ortega, and Pierre Vandergheynst. The emerging field of signal processing on graphs: Extending high-dimensional data analysis to networks and other irregular domains. *IEEE signal processing magazine*, 30(3):83–98, 2013.
- [44] Daniel A Spielman and Shang-Hua Teng. Spectral sparsification of graphs. *SIAM Journal on Computing*, 40(4):981–1025, 2011.
- [45] Fei Sun, Jun Liu, Jian Wu, Changhua Pei, Xiao Lin, Wenwu Ou, and Peng Jiang. Bert4rec: Sequential recommendation with bidirectional encoder representations from transformer. In *Proceedings of the 28th ACM international conference on information and knowledge management*, pages 1441–1450, 2019.
- [46] Nicolas Tremblay, Paulo Gonçalves, and Pierre Borgnat. Chapter 11 - design of graph filters and filterbanks. In Petar M. Djurić and Cédric Richard, editors, *Cooperative and Graph Signal Processing*. Academic Press, 2018.
- [47] Ulrike Von Luxburg. A tutorial on spectral clustering. *Statistics and computing*, 17:395–416, 2007.
- [48] Wenjie Wang, Yiyang Xu, Fuli Feng, Xinyu Lin, Xiangnan He, and Tat-Seng Chua. Diffusion recommender model. In *Proceedings of the 46th International ACM SIGIR Conference on Research and Development in Information Retrieval*, pages 832–841, 2023.
- [49] Xiang Wang, Xiangnan He, Meng Wang, Fuli Feng, and Tat-Seng Chua. Neural graph collaborative filtering. In *Proceedings of the 42nd international ACM SIGIR conference on Research and development in Information Retrieval*, pages 165–174, 2019.
- [50] Xiang Wang, Hongye Jin, An Zhang, Xiangnan He, Tong Xu, and Tat-Seng Chua. Disentangled graph collaborative filtering. In *Proceedings of the 43rd international ACM SIGIR conference on research and development in information retrieval*, pages 1001–1010, 2020.
- [51] Wei Wu, Chao Wang, Dazhong Shen, Chuan Qin, Liyi Chen, and Hui Xiong. Afdgcf: Adaptive feature de-correlation graph collaborative filtering for recommendations. In *Proceedings of the 47th International ACM SIGIR Conference on Research and Development in Information Retrieval*, pages 1242–1252, 2024.
- [52] Jiafeng Xia, Dongsheng Li, Hansu Gu, Tun Lu, Peng Zhang, Li Shang, and Ning Gu. Frequency-aware graph signal processing for collaborative filtering. *arXiv preprint arXiv:2402.08426*, 2024.
- [53] Jiafeng Xia, Dongsheng Li, Hansu Gu, Tun Lu, Peng Zhang, Li Shang, and Ning Gu. Hierarchical graph signal processing for collaborative filtering. In *Proceedings of the ACM Web Conference 2024*, pages 3229–3240, 2024.
- [54] Rui Xia, Yanhua Cheng, Yongxiang Tang, Xiaocheng Liu, Xialong Liu, Lisong Wang, and Peng Jiang. S-diff: An anisotropic diffusion model for collaborative filtering in spectral domain. In *Proceedings of the Eighteenth ACM International Conference on Web Search and Data Mining*, pages 70–78, 2025.
- [55] Rex Ying, Ruining He, Kaifeng Chen, Pong Eksombatchai, William L Hamilton, and Jure Leskovec. Graph convolutional neural networks for web-scale recommender systems. In *Proceedings of the 24th ACM SIGKDD international conference on knowledge discovery & data mining*, pages 974–983, 2018.
- [56] An Zhang, Wenchang Ma, Pengbo Wei, Leheng Sheng, and Xiang Wang. General debiasing for graph-based collaborative filtering via adversarial graph dropout. In *Proceedings of the ACM Web Conference 2024*, pages 3864–3875, 2024.
- [57] Shengzhe Zhang, Liyi Chen, Chao Wang, Shuangli Li, and Hui Xiong. Temporal graph contrastive learning for sequential recommendation. In *Proceedings of the AAAI Conference on Artificial Intelligence*, volume 38, pages 9359–9367, 2024.
- [58] Yifei Zhang, Hao Zhu, Zixing Song, Piotr Koniusz, Irwin King, et al. Mitigating the popularity bias of graph collaborative filtering: A dimensional collapse perspective. *Advances in Neural Information Processing Systems*, 36:67533–67550, 2023.

- [59] Yijie Zhang, Yuanchen Bei, Hao Chen, Qijie Shen, Zheng Yuan, Huan Gong, Senzhang Wang, Feiran Huang, and Xiao Huang. Multi-behavior collaborative filtering with partial order graph convolutional networks. In *Proceedings of the 30th ACM SIGKDD Conference on Knowledge Discovery and Data Mining*, pages 6257–6268, 2024.
- [60] Lei Zheng, Chun-Ta Lu, Fei Jiang, Jiawei Zhang, and Philip S Yu. Spectral collaborative filtering. In *Proceedings of the 12th ACM conference on recommender systems*, pages 311–319, 2018.
- [61] Yunqin Zhu, Chao Wang, Qi Zhang, and Hui Xiong. Graph signal diffusion model for collaborative filtering. In *Proceedings of the 47th International ACM SIGIR Conference on Research and Development in Information Retrieval*, pages 1380–1390, 2024.

Appendices

This supplementary material provides detailed information that complements our main paper. It includes formal notation definitions, theoretical analysis, algorithmic details, computational complexity analysis, and experimental information to support reproducibility.

A Table of Notations

We summarize the key notations used throughout this paper in Table 7.

Table 7: Summary of Notations

Notation	Description
<i>Input Data Representations</i>	
\mathcal{U}, \mathcal{I}	Set of users and items, respectively
\mathcal{D}	Historical interactions as (u, i, t) triplets
$\mathbf{X} \in \{0, 1\}^{m \times n}$	Binary user-item interaction matrix
\mathcal{S}_u	Time-ordered sequence of items for user u
<i>Graph Construction</i>	
\mathbf{S}	Initial directed item transition matrix from \mathcal{S}_u
\mathbf{S}'	Symmetric item connectivity graph derived from \mathbf{S}
α, d	Diffusion decay factor and depth
$\mathbf{S}^{(d)}$	Multi-hop diffusion matrix from \mathbf{S}' up to depth d
$\tilde{\mathbf{S}}$	Normalized diffusion matrix derived from $\mathbf{S}^{(d)}$
\mathbf{A}	Unified user-item adjacency matrix
\mathbf{L}	Normalized Laplacian matrix
<i>Spectral Filtering</i>	
$\mathbf{U}, \mathbf{\Lambda}$	Matrices of eigenvectors and eigenvalues of \mathbf{L} , respectively
r	Number of eigenvectors in truncated decomposition
$g_{\text{BP}}(\lambda)$	Gaussian bandpass filter kernel
c, w	Center and width of bandpass filter
\mathbf{F}_{BP}	Bandpass filtered user-item signal
\mathbf{F}_{LP}	Lowpass filtered user-item signal
ϕ	Fusion parameter balancing filter components
\mathbf{Y}	Final prediction matrix

B Algorithmic Details

B.1 GSPRec Algorithm

The full end-to-end procedure of our method is outlined in Algorithm 1. It summarizes the construction of the sequential graph encoding, Laplacian computation, spectral filtering, and final score generation.

B.2 Proof of Proposition 2: Laplacian Validity

Proof. We first establish properties of the adjacency matrix $\mathbf{A} \in \mathbb{R}^{(m+n) \times (m+n)}$, defined as:

$$\mathbf{A} = \begin{pmatrix} \mathbf{0}_{m \times m} & \mathbf{X} \\ \mathbf{X}^T & \tilde{\mathbf{S}} \end{pmatrix} \quad (12)$$

where $\mathbf{X} \in \{0, 1\}^{m \times n}$ (the binary user-item interaction matrix) and $\tilde{\mathbf{S}} = \mathbf{D}_S^{-1/2} \mathbf{S}^{(d)} \mathbf{D}_S^{-1/2} \in \mathbb{R}^{n \times n}$ (the normalized sequence-derived item-item graph, with $\mathbf{S}^{(d)}$ being the diffused matrix from Eq. 2).

Lemma 4. *The adjacency matrix \mathbf{A} is symmetric and non-negative.*

Algorithm 1: GSPRec

Input: Interaction set $\mathcal{D} = \{(u, i, t)\}$, diffusion order d , decay factor α , filter parameters (c, w) , fusion weight ϕ

Output: Predicted score matrix $\mathbf{Y} \in \mathbb{R}^{m \times n}$

// Graph Construction

$\mathbf{X} \leftarrow$ Binary user-item matrix from \mathcal{D}

$\mathcal{S}_u \leftarrow$ Chronologically sorted item sequences per user

$\mathbf{S} \leftarrow$ Initial directed item transition matrix from \mathcal{S}_u (where $S_{ij} = 1$ if $i \rightarrow j$)

$\mathbf{S}' \leftarrow$ Symmetrize(\mathbf{S}) // $S'_{ij} = 1$ if $S_{ij} = 1$ or $S_{ji} = 1$

$\mathbf{S}^{(d)} \leftarrow \sum_{k=1}^d \alpha^{k-1} (\mathbf{S}')^k$ // Exponential diffusion on symmetric \mathbf{S}'

$\tilde{\mathbf{S}} \leftarrow \mathbf{D}_S^{-1/2} \mathbf{S}^{(d)} \mathbf{D}_S^{-1/2}$ // where $\mathbf{D}_S = \text{diag}(\mathbf{S}^{(d)} \mathbf{1}_n)$

$\mathbf{A} \leftarrow \begin{bmatrix} \mathbf{0} & \mathbf{X} \\ \mathbf{X}^\top & \tilde{\mathbf{S}} \end{bmatrix}$

$\mathbf{D} \leftarrow \text{diag}(\mathbf{A} \mathbf{1})$

$\mathbf{L} \leftarrow \mathbf{I} - \mathbf{D}^{-1/2} \mathbf{A} \mathbf{D}^{-1/2}$

$[\mathbf{U}, \mathbf{\Lambda}] \leftarrow$ Eigendecomposition of \mathbf{L}

// Frequency-Aware Spectral Filtering

$\bar{\lambda} \leftarrow$ Diagonal entries of $\mathbf{\Lambda}$

$\mathbf{G}_{\text{BP}} \leftarrow \text{diag} \left(\exp \left(-\frac{(\bar{\lambda} - c)^2}{w} \right) \right)$ // Gaussian band-pass

$\mathbf{F}_{\text{BP}} \leftarrow \mathbf{X} \mathbf{D}_I^{-1/2} \mathbf{U} \mathbf{G}_{\text{BP}} \mathbf{U}^\top \mathbf{D}_I^{-1/2}$

// Low-Pass Filtering

$\tilde{\mathbf{X}}_U \leftarrow \mathbf{D}_U^{-1/2} \mathbf{X}$ // where $\mathbf{D}_U = \text{diag}(\mathbf{X} \mathbf{1}_n)$, $\mathbf{D}_I = \text{diag}(\mathbf{X}^\top \mathbf{1}_m)$

$\mathbf{C}_U \leftarrow \tilde{\mathbf{X}}_U \tilde{\mathbf{X}}_U^\top$

$\mathbf{X}_b \leftarrow [\mathbf{C}_U, \mathbf{X}]$

$\mathbf{D}_b \leftarrow \text{diag}(\mathbf{X}_b^\top \mathbf{1})$

$\mathbf{F}_{\text{LP}} \leftarrow \mathbf{X}_b \mathbf{D}_b^{-1/2} \mathbf{U} \mathbf{U}^\top \mathbf{D}_b^{1/2}$

$\mathbf{F}_{\text{LP}} \leftarrow \mathbf{F}_{\text{LP}}[:, m:]$ // Select only item columns

// Fusion and Output

$\mathbf{Y} \leftarrow \phi \cdot \mathbf{F}_{\text{BP}} + (1 - \phi) \cdot \mathbf{F}_{\text{LP}}$

return \mathbf{Y}

Proof of Lemma 4. To prove symmetry of \mathbf{A} , we note:

$$\mathbf{A}^T = \begin{pmatrix} \mathbf{0}_{m \times m}^T & (\mathbf{X}^T)^T \\ \mathbf{X}^T & \tilde{\mathbf{S}}^T \end{pmatrix} \quad (13)$$

$$= \begin{pmatrix} \mathbf{0}_{m \times m} & \mathbf{X} \\ \mathbf{X}^T & \tilde{\mathbf{S}} \end{pmatrix} = \mathbf{A} \quad (14)$$

This equality holds because $\mathbf{0}_{m \times m}$ is symmetric, $(\mathbf{X}^T)^T = \mathbf{X}$, and $\tilde{\mathbf{S}}^T = \tilde{\mathbf{S}}$. The matrix $\tilde{\mathbf{S}}$ is symmetric by construction: the base matrix \mathbf{S}' used in the diffusion is symmetric, thus $\mathbf{S}^{(d)}$ (from Eq. 2) is symmetric, and the symmetric normalization (Eq. 3) preserves this symmetry.

For non-negativity of \mathbf{A} , we show all its elements are non-negative:

- $\mathbf{X} \in \{0, 1\}^{m \times n}$ by definition, so its elements are ≥ 0 . Thus, $\mathbf{X} \geq 0$ and $\mathbf{X}^T \geq 0$.
- For $\tilde{\mathbf{S}}$: The initial directed transition matrix \mathbf{S} has $s_{ij} \in \{0, 1\}$, so $\mathbf{S} \geq 0$. The symmetric base graph \mathbf{S}' is constructed from \mathbf{S} such that its entries $s'_{ij} \in \{0, 1\}$, so $\mathbf{S}' \geq 0$. Given $\mathbf{S}' \geq 0$ and the decay factor $\alpha \in (0, 1) > 0$, each power $(\mathbf{S}')^k$ in the diffusion sum will have non-negative entries. Therefore, $\mathbf{S}^{(d)} = \sum_{k=1}^d \alpha^{k-1} (\mathbf{S}')^k$ (Eq. 2) will also have non-negative entries, i.e., $\mathbf{S}^{(d)} \geq 0$. The degree matrix $\mathbf{D}_S = \text{diag}(\mathbf{S}^{(d)} \mathbf{1}_n)$ will have non-negative diagonal entries. For non-isolated nodes in the graph represented by $\mathbf{S}^{(d)}$,

these entries will be positive, making $\mathbf{D}_S^{-1/2}$ well-defined with non-negative real entries. Hence, $\tilde{\mathbf{S}} = \mathbf{D}_S^{-1/2} \mathbf{S}^{(d)} \mathbf{D}_S^{-1/2} \geq 0$.

Therefore, \mathbf{A} is both symmetric and non-negative. \square

Given that \mathbf{A} is symmetric and non-negative (by Lemma 4), and its degree matrix $\mathbf{D} = \text{diag}(\mathbf{A}\mathbf{1})$, the normalized Laplacian is $\mathbf{L} = \mathbf{I} - \mathbf{D}^{-1/2} \mathbf{A} \mathbf{D}^{-1/2}$ (Eq. 6). We apply Theorem 5:

Theorem 5 (Properties of Normalized Laplacian (Chung, 1997 [6])). *For a symmetric, non-negative adjacency matrix \mathbf{A} with degree matrix \mathbf{D} , the normalized Laplacian $\mathbf{L} = \mathbf{I} - \mathbf{D}^{-1/2} \mathbf{A} \mathbf{D}^{-1/2}$ satisfies: (1) \mathbf{L} is real and symmetric. (2) \mathbf{L} is positive semi-definite. (3) All eigenvalues of \mathbf{L} lie in $[0, 2]$.*

Applying Theorem 5 directly to our \mathbf{A} and \mathbf{L} concludes that \mathbf{L} is symmetric, positive semi-definite, and has eigenvalues in $[0, 2]$. \square

C Theoretical Analysis of Spectral Bands

The concentration of user-specific patterns in mid-frequency components can be understood through the lens of graph signal smoothness. Low-frequency components correspond to signals that are smooth across the graph, capturing global popularity trends that vary slowly across the user-item structure. High-frequency components often represent noise or sparse outlier preferences.

Mid-frequency components represent a balance where signals vary moderately across local graph neighborhoods - precisely the pattern exhibited by personalized preferences that differ between user communities but show consistency within them. This aligns with previous findings in spectral clustering [47] and network community detection [31], where mid-frequency eigenvectors have been shown to encode community structure.

We can formalize this intuition through the concept of total variation of a signal [43]. Given a signal \mathbf{f} on a graph with Laplacian \mathbf{L} , the quadratic form $\mathbf{f}^T \mathbf{L} \mathbf{f}$ measures how smoothly the signal varies across the graph. For the eigenvectors \mathbf{u}_i of \mathbf{L} , we have $\mathbf{u}_i^T \mathbf{L} \mathbf{u}_i = \lambda_i$, where λ_i is the corresponding eigenvalue.

User preference signals can be decomposed into these eigenvectors:

$$\mathbf{f} = \sum_{i=1}^{m+n} \alpha_i \mathbf{u}_i \quad (15)$$

In our empirical analysis across datasets, we consistently observe that coefficients α_i corresponding to mid-frequency components ($0.3 < \lambda_i < 0.8$) have significantly higher magnitude for user-specific preference patterns compared to global trends. This provides empirical validation of our theoretical understanding of spectral representation in recommendation graphs.

D Computational Complexity Analysis

We analyze the computational complexity of GSPRec with m users, n items, $|\mathcal{D}|$ interactions, diffusion depth d , and r eigenvectors.

D.1 Time Complexity

The time complexity of key components is:

- **Graph Construction:** $O(|\mathcal{D}| + d \cdot \text{nnz}(\mathbf{S}') \cdot n)$ for building and diffusing the sequential transition matrix.
- **Eigendecomposition:** $O(r \cdot (m+n)^2)$ for computing the r smallest eigenvectors of the Laplacian.
- **Spectral Filtering:** $O(|\mathcal{D}| \cdot r + (m+n) \cdot r^2)$ for applying band-pass and low-pass filters.

The overall time complexity is dominated by the eigendecomposition step: $O(r \cdot (m + n)^2)$. For sparse interaction data and $r \ll (m + n)$, the algorithm remains computationally tractable.

D.2 Space Complexity

The space requirements are:

- **Input Data:** $O(|\mathcal{D}| + \text{nnz}(\mathbf{S}^{(d)}))$ for storing user-item interactions and sequential transitions.
- **Spectral Representation:** $O(r \cdot (m + n))$ for storing eigenvectors.
- **Output:** $O(m \cdot n)$ for the filtered results and final predictions.

The overall space complexity is $O(|\mathcal{D}| + \text{nnz}(\mathbf{S}^{(d)}) + r \cdot (m + n) + m \cdot n)$, which is manageable for sparse real-world recommendation datasets where $|\mathcal{D}| \ll m \cdot n$ and $\text{nnz}(\mathbf{S}^{(d)}) \ll n^2$.

In practice, the algorithm can be further optimized through sparse matrix operations, approximate eigendecomposition methods, and parallelization of filtering operations.

E Baseline Details

We compare GSPRec with a comprehensive set of baselines representing both GCN-based and GSP-based CF methods:

GCN-based CF Methods:

- **LightGCN** [14] simplifies GCN for recommendation by removing feature transformation and non-linear activation, retaining only essential neighborhood aggregation.
- **LR-GCCF** [4] introduces residual connections to graph convolutional networks for improving recommendation performance.
- **IMP-GCN** [23] propagates information in user sub-graphs to reduce the impact of noise and alleviate the over-smoothing problem.
- **SimpleX** [28] focuses on optimizing loss function and negative sampling strategies.
- **UltraGCN** [29] approximates infinite-layer graph convolutions via constraint loss and flexible edge weight assignment.

GSP-based CF Methods:

- **GF-CF** [42] integrates linear and ideal low-pass filters to model user preferences.
- **PGSP** [25] uses a mixed-frequency low-pass filter over personalized graph signals.
- **FaGSP** [52] employs Cascaded and Parallel Filter Modules for user preference modeling.
- **HiGSP** [53] adopts cluster-wise and globally-aware filters to recognize unique and general interaction patterns.

For comprehensive evaluation, we report results for LR-GCCF, IMP-GCN, SimpleX, UltraGCN, and GF-CF as presented in [53, 52], which used identical dataset preprocessing and evaluation protocols.

F Reproducibility

To improve reproducibility, we provide the complete algorithm of GSPRec in Algorithm 1, which details the graph construction, spectral decomposition, and dual filtering processes. The optimal hyperparameters for all experimental datasets are summarized in Table 3. For implementation, we process datasets following the procedure described in Section 4.1, which involves splitting datasets in an 8:2 ratio for training/testing, with 10% of the training set used for validation. When implementing GSPRec, the key parameter settings are:

- Diffusion depth $d = 2$ and decay factor $\alpha = 0.4$ for sequential graph construction

- Dataset-specific eigenvector count r , band-pass center c , width w , and fusion weight ϕ as specified in Table 3

For evaluation, we follow the protocol detailed in Section 4.1, using NDCG and MRR metrics at $k \in \{5, 10, 20\}$ after excluding previously interacted items.

F.1 Computational Resources

Experiments were conducted on a system with AMD EPYC processors and NVIDIA RTX A6000 GPUs. The computational requirements varied with dataset size and the number of eigenvectors used. The eigendecomposition step is the primary computational bottleneck as identified in our complexity analysis (Appendix D). For benchmark datasets used in our experiments, the runtime and memory requirements were reasonable, allowing for comprehensive evaluation on standard research hardware. Our experimental protocol, including parameter tuning and ablation studies, involved multiple runs for each configuration to ensure statistical significance.

F.2 Scaling to Large-Scale Systems

For industrial-scale applications with millions of users and items, we propose three optimization strategies:

F.2.1 Approximate Eigendecomposition

The dominant computational bottleneck can be addressed using the Nyström method [8] or randomized SVD approaches [11], reducing complexity from $O(r(m+n)^2)$ to $O(r^2(m+n))$ (or better, depending on specific variant, e.g., linear in $(m+n)$ for matrix-vector products), with minimal performance impact.

F.2.2 Graph Sparsification

For large-scale graphs, we can apply spectral sparsification techniques [44] that preserve the essential spectral properties while reducing edge density, accelerating both graph construction and eigendecomposition.

F.2.3 Incremental Updates

In production environments, the full spectral decomposition need not be recomputed for each recommendation. We propose an incremental update scheme where the spectral components are updated periodically while incremental preference updates can be applied in real-time.

G Mathematical Analysis of Bandpass Filtering

We provide mathematical justification for our bandpass filtering approach and its relevance to recommendation systems. Our Gaussian kernel on the graph Laplacian eigenspectrum is defined as in Equation 7.

$$g(\lambda) = \exp\left(-\frac{(\bar{\lambda} - c)^2}{w}\right), \quad \bar{\lambda} = \frac{\lambda - \lambda_{\min}}{\lambda_{\max} - \lambda_{\min}}$$

This satisfies the formal definition of a bandpass filter: it achieves maximum response when $\bar{\lambda} = c$ (which corresponds to $\lambda_c = c(\lambda_{\max} - \lambda_{\min}) + \lambda_{\min}$ in the original eigenvalue domain) and attenuates components with eigenvalues far from λ_c . For our normalized Laplacian with original eigenvalues $\lambda \in [0, 2]$ (so $\lambda_{\min} \approx 0, \lambda_{\max} \approx 2$), setting $c \in (0, 1)$ (the center in the normalized $\bar{\lambda} \in [0, 1]$ domain) ensures the filter passes a band of mid-range eigenvalues while attenuating both low and high extremes. When applied to user preference signals decomposed as $\mathbf{x} = \sum_{i=1}^{m+n} \alpha_i \mathbf{u}_i$, the filtered output $\mathbf{y} = \mathbf{U} \text{diag}(g(\mathbf{\Lambda})) \mathbf{U}^T \mathbf{x}$ selectively preserves components $\alpha_i \mathbf{u}_i$ where the eigenvalue λ_i (corresponding to \mathbf{u}_i) results in a high $g(\lambda_i)$ value.

Our empirical analysis across recommendation datasets reveals that coefficients α_i corresponding to intermediate eigenvalues ($0.3 < \lambda_i < 0.8$, assuming λ_i are original eigenvalues in $[0, 2]$) have

higher magnitude for user-specific preference patterns compared to global trends. This confirms that mid-frequency components encode valuable personalization signals that traditional low-pass approaches would suppress.

Table 6 provides quantitative evidence of this phenomenon: while low-pass filtering captures popularity trends, our bandpass approach more effectively preserves the user-specific patterns essential for accurate personalized recommendations.